Human Molecular Genetics, 2004, Vol. 13, No. 14 **1505–1514**
DOI: 10.1093/hmg/ddh163
Advance Access published on May 26, 2004

The subcellular localization of the ChoRE-binding protein, encoded by the Williams–Beuren syndrome critical region gene 14, is regulated by 14-3-3

Giuseppe Merla[†], Cédric Howald, Stylianos E. Antonarakis and Alexandre Reymond[*,‡]

Department of Genetic Medicine and Development, University of Geneva Medical School, Geneva, Switzerland

Received March 22, 2004; Revised and Accepted May 13, 2004

The Williams–Beuren syndrome (WBS) is a contiguous gene syndrome caused by chromosomal rearrangements at chromosome band 7q11.23. Several endocrine phenotypes, in particular impaired glucose tolerance and silent diabetes, have been described for this clinically complex disorder. The *WBSCR14* gene, one of the genes mapping to the WBS critical region, encodes a member of the basic-helix-loop-helix leucine zipper family of transcription factors, which dimerizes with the Max-like protein, Mlx. This heterodimeric complex binds and activates, in a glucose-dependent manner, carbohydrate response element (ChoRE) motifs in the promoter of lipogenic enzymes. We identified five novel WBSCR14-interacting proteins, four 14-3-3 isotypes and NIF3L1, which form a single polypeptide complex in mammalian cells. Phosphatase treatment abrogates the association between WBSCR14 and 14-3-3, as shown previously for multiple 14-3-3 interactors. WBSCR14 is exported actively from the nucleus through a CRM1-dependent mechanism. This translocation is contingent upon the ability to bind 14-3-3. Through this mechanism the 14-3-3 isotypes directly affect the WBSCR14:Mlx complexes, which activate the transcription of lipogenic genes.

INTRODUCTION

In mammals, the liver is the principal organ responsible for the conversion of excess dietary carbohydrates to triglycerides, the predominant storage form of energy. Elevated glucose levels in the liver lead to either gene transcriptional induction or post-translational activation of several key enzymes of glycolysis and lipogenesis, including fatty acid synthase, acetylCoA carboxylase and L-type pyruvate kinase (LPK) (1–3). The carbohydrate responsive element binding protein (ChREBP) transcription factor, the rat ortholog of Williams–Beuren syndrome critical region gene 14 [hereafter named WBSCR14 following recommendation of the HUGO Gene Nomenclature Committee (4)] is expressed under high-glucose diet and inhibited under high-fat diet in primary cultured hepatocytes. Its overexpression in these cells results in increased transcription of the *LPK* gene through direct binding of the carbohydrate response element (ChoRE) of the LPK promoter (5–9). The *WBSCR14* gene encodes a member of the basic-helix-loop-helix leucine zipper (bHLHZip) family of transcription factors (10), which dimerizes with the Max-like protein, Mlx, to bind E-box motifs in the promoter region of target genes (7,11). High-glucose level activates the nuclear translocation and the DNA-binding activity of rat WBSCR14, through Ser^{196} and Thr^{666} dephosphorylation by xylulose 5-phosphate-activated protein phosphatase 2A in primary hepatocytes (12). Conversely, glucagon and fatty acids increase the level of AMP and cAMP in hepatocytes activating AMPK and/or PKA, which results in the phosphorylation of WBSCR14 at residue Ser^{568} and inhibition of its DNA-binding activity (5,6,9,12). Recent observations demonstrated that rat WBSCR14 plays also an essential role in the regulation of other lipogenic enzymes, besides LPK, involved in glucose and lipid metabolism (12–14).

Williams–Beuren syndrome patients (WBS, OMIM#194050) are hemizygous for the *WBSCR14* gene (8,15). WBS is a neurodevelopmental disorder characterized by numerous

*To whom correspondence should be addressed at: Department of Genetic Medicine and Development, University of Geneva Medical School, CMU, 1, rue Michel Servet, 1211 Geneva 4, Switzerland. Tel: +41 223795719; Fax: + 41 223795706; Email: alexandre.reymond@medecine.unige.ch
[†]Present address: Servizio Genetica Medica, IRCCS 'Casa Sollievo della Sofferenza', San Giovanni Rotondo, Italy.
[‡]Present address: Center for Integrative Genomics, University of Lausanne, Lausanne, Switzerland.

clinical aspects including mental retardation with unique cognitive and personality profile (16,17). The cognitive hallmark of WBS individuals is dissociation between language (relative strength) and spatial cognition (profound impairment). The WBS incidence is estimated at 1/20 000 and sporadic *de novo* inheritance is usual. The molecular basis of the syndrome is a heterozygous ~1.5 Mb microdeletion or rarely an inversion at chromosome band 7q11.23. While our understanding of the etiology of WBS has improved greatly, the molecular basis of all except the cardiovascular phenotype remains unknown (18–22). Approximately 75% of the WBS patients show impaired glucose tolerance (IGT) or silent diabetes (17). The elevated glucose levels of these patients suggest that glucose uptake plays a role in the occurrence of these phenotypes. We surmise that they could be related to WBSCR14 hemizygosity and to the ability of this transcription factor to control the expression of lipogenic enzymes.

We performed a yeast two-hybrid selection to identify proteins that regulate the function of WBSCR14. In this report, we describe five new *Wbscr14*-interactors. These proteins participate in the regulation of WBSCR14-dependent transcription, through control of the subcellular localization of the ChoRE-binding protein.

RESULTS

Two-hybrid selection

To identify new proteins that interact with WBSCR14, and potentially regulate its nuclear translocation, we performed a yeast two-hybrid selection using two human cDNA libraries (from HeLa cells and human fetal brain). A fusion between LexA and mouse *Wbscr14*-ζ residues 81–297 was used as bait. This construct encompasses the protein amino-terminal domain of repression (PADRE, Fig. 1A), which was shown to repress transcription when fused to the GAL4 DNA binding domain (7). Repression was accomplished through retention of the GAL4 moiety outside of the nucleus (23). This selection allowed us to identify five potential novel *Wbscr14*-interactors.

Wbscr14 interacts with 14-3-3

Four of these interactors were cloned from both screened libraries. They correspond to different 14-3-3 isotypes, specifically 14-3-3 β, γ, ζ and θ. Because large proteins with multiple 14-3-3 docking sites have been described (24), we tested if more than one 14-3-3-binding moiety existed on the *Wbscr14* protein using the interaction–mating technology (25). A panel of overlapping *Wbscr14* peptides expressed as fusion proteins with the LexA–DNA binding domain (bait) was tested for interaction with 14-3-3 β, ζ and θ and Mlx-α fused to the B42-acidic moiety (prey). Consistent with previous results, *Wbscr14*, bHLHZip (584–765), WMC (737–864) and PADRE (1–146 and 81–297) domains interact with Mlx (7) and 14-3-3 β, ζ and θ isotypes (see above), respectively. In addition, we found that 14-3-3 β and ζ also interact with the *Wbscr14* 584–765 peptide, suggesting that two independent 14-3-3-binding moieties are present on the *Wbscr14* protein (Fig. 1A and B).

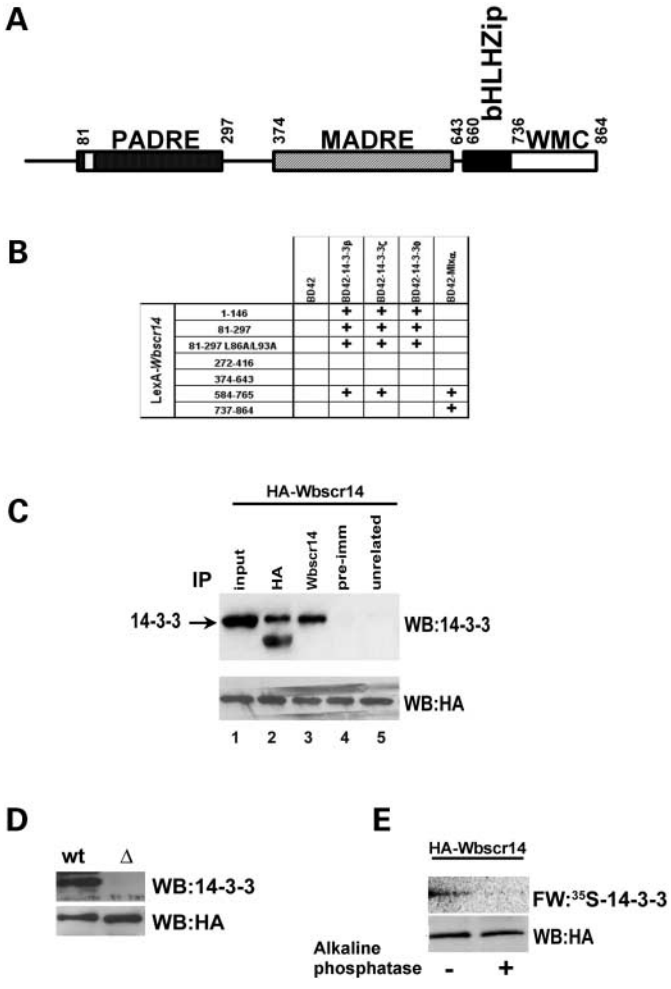

Figure 1. Phosphorylated *Wbscr14* interacts with 14-3-3. (**A**) Schematic representation of the *Wbscr14*-ζ domains (defined in 7). The PADRE was used as bait in the two-hybrid selection. MADRE: middle activation domain as in RelB; bHLHZip: basic helix-loop-helix leucine zipper domain; WMC: WBSCR14-Mlx C-tail homologous domain. The white box within the PADRE domain represents the NES domain. (**B**) Interaction–mating assays between EGY42 bait strains carrying LexA fusions to overlapping *Wbscr14*-ζ peptides and EGY48 derivatives that contain B42 fusions to human Mlx-β and 14-3-3 β, ζ and θ isotypes. The '+' signs denote interaction as measured by lacZ expression and LEU2 expression on galactose/raffinose media, whereas empty cells indicate no interaction. (**C**) *Wbscr14* interacts with endogenous 14-3-3. COS-7 cells were transfected with plasmids expressing HA–*Wbscr14*-ζ. Lysates were immunoprecipitated with anti-HA mAb (lane 2), anti-*Wbscr14* (3), its preimmune counterpart (4) or an unrelated antisera (5) as specified above. Immunoprecipitated complexes were revealed by immunoblotting with an anti-14-3-3 (top panel) or an anti-HA (bottom panel) antibody. The anti-14-3-3 antibody used recognizes all seven 14-3-3 isotypes. Abbreviations: WB, western blotting with specified antibody; IP, immunoprecipitation with specified antibody. (**D**) *Wbscr14* residues 117–133 are essential for 14-3-3-binding. HA–*Wbscr14*-ζ (left lane) and HA–*Wbscr14*-ζ Δ117–133 (right lane) were transfected transiently in COS-7 cells. Lysates were immunoprecipitated with an anti-HA mAb and revealed by immunoblotting with an anti-14-3-3 (top panel) or an anti-HA (bottom panel) antibody. (**E**) Dephosphorylation of *Wbscr14* disrupts its interaction with 14-3-3. The anti-*Wbscr14* immunoprecipitate from (C) was dephosphorylated with alkaline phosphatase (right lane) or mock treated (left lane) and probed for binding to *in vitro* labeled and transcribed 14-3-3 θ (top panel). Stripping and reprobing the membrane with an anti-HA antibody showed that similar amounts of *Wbscr14* protein were used in each lanes (bottom panel). Abbreviations: FW, far western blotting with specified interactor.

To determine if *Wbscr14* binds to the COS-7 endogenous 14-3-3 isotypes, total cell lysates of HA–*Wbscr14*-ζ transfected cells were immunoprecipitated with immune and pre-immune sera raised against *Wbscr14*, with immune sera raised against an unrelated protein or with an anti-HA monoclonal antibody. The precipitated proteins were separated by gel electrophoresis and subjected to immunoblot analysis using antibodies reactive against 14-3-3 mammalian isotypes. The 14-3-3 proteins were found in the anti-HA and anti-*Wbscr14* immunoprecipitates, but not in the controls (Fig. 1C, compare lanes 2 and 3 with 4 and 5). Similarly, we could immunoprecipitate complexes containing endogenous 14-3-3 and transfected HA–*Wbscr14*-ζ proteins from 293T cells (data not shown). This interaction is not specific to certain isotypes, as HA–*Wbscr14* protein co-precipitates with 14-3-3 β, γ/η, ε, ζ and θ isotypes (data not shown). Interaction with the σ (stratifin) isotype could not be tested, as we were unable to detect this form in COS-7 cells (data not shown).

To better define the *Wbscr14* N-terminal 14-3-3-binding moiety, we created three deletion mutants: HA–*Wbscr14*-ζ Δ86–95, Δ103–114 and Δ117–133. These deletions span the *Wbscr14* PADRE domain essential for the 14-3-3-interaction. Deletion of residues 117–133 completely abrogates interaction with 14-3-3, whereas the other mutants retain their affinity (Fig. 1D and data not shown). This result also indicates that the second 14-3-3-binding site of *Wbscr14* (see above) might correspond to a low affinity site not essential for the formation of the complex, but only for its stability (24).

Because 14-3-3 proteins are known to often bind proteins containing phosphothreonine or phosphoserine motifs (24), we questioned whether the phosphorylation status of *Wbscr14* would influence 14-3-3-binding. Membrane-fixed mock and alkaline phosphatase treated HA–*Wbscr14*-ζ proteins were tested for binding to *in vitro* translated and labeled 14-3-3 θ. The phosphatase treatment abrogates *Wbscr14*:14-3-3 θ association suggesting that phosphorylation of the bHLHZip transcription factor is required for interaction (Fig. 1E). As no sequence resembling a 14-3-3 binding consensus maps to the region between residues 117 and 133 of *Wbscr14*-ζ, we surmise that the phosphorylation-dependent interaction observed occurs indirectly through a protein present in rabbit reticulocyte lysates that bridges 14-3-3 and *Wbscr14*. Alternatively, the phosphorylation status of *Wbscr14* could influence the folding, hence abolishing the interaction with 14-3-3.

Recently, the phosphorylation status of residues S196, S568, S626 and T666 was shown to play a crucial role in the nuclear localization and DNA-binding activity of the *Wbscr14* rat ortholog in primary rat hepatocytes (6). We tested whether mutants mimicking the unphosphorylated state of these and the S140 residues were still able to interact with the 14-3-3 protein. None of the single mutants, *Wbscr14*-ζ S140A, S196A, S568A, S626A and T666A, showed an impaired affinity for 14-3-3 (Supplementary Material, Fig. S1A). We next tested whether phosphorylation of these residues exerts a cooperative effect on the interaction. For this, we created a quadruple mutant (S196A/S568A/S626A/T666A) and investigated its ability to interact with 14-3-3. Again, this mutant shows no alteration in its affinity for 14-3-3 (Supplementary Material, Fig. S1A). These results confirm that the phosphorylation status of these residues are not involved directly in the ability of *Wbscr14*-ζ to interact with 14-3-3.

14-3-3 θ expression specifically represses the transcriptional activity of *Wbscr14-ζ*

As heterodimers formed between Wbscr14 and Mlx activate the transcription of an E-box driven Luciferase construct and the *LPK* gene promoter (G. Merla and A. Reymond, unpublished data) (14), we inquired whether 14-3-3 proteins could act as regulators of Wbscr14-ζ transcriptional activity. Expression of increasing amounts of 14-3-3 θ leads to the repression of *Wbscr14*-ζ:Mlx-mediated transcription in a dose-dependent manner, indicating that 14-3-3 θ controls the *Wbscr14* activity (Fig. 2A and B). To confirm the specificity of this effect, we repeated the experiment using *Wbscr14*-ζ Δ117–133, a *Wbscr14* mutant heterodimerizing with Mlx and activating transcription of E-box-driven reporters, yet unable to bind 14-3-3 (see above and Fig. 1D). This mutant shows a lower relative activity when compared with its wild-type counterpart (Fig. 2A), probably reflecting a diminution of the stability of the protein as seen by western blot (data not shown). The results show no influence of 14-3-3 on the transcriptional activation mediated by *Wbscr14*-ζ Δ117–133:Mlx complex demonstrating that 14-3-3 specifically regulates Wbscr14 transcription (Fig. 2A).

Wbscr14, *NIF3L1* and 14-3-3 form a complex

The two-hybrid screening of the human fetal brain library revealed a fifth potential *Wbscr14*-interactor besides 14-3-3 isotypes. We isolated two identical clones corresponding to the entire open reading frame of an as yet unidentified Ngg1-interacting factor 3-like 1 (NIF3L1) isoform, we named NIF3L1-γ (AY251944). NIF3L1-γ shares with the original NIF3L1 seven-exon transcript [which we named isoform α; AF283538; (26)] the first two coding exons, but differs by skipping exons 5 and 6 and using cryptic donor and acceptor sites in exon 4 and 7, respectively (Fig. 3A). NIF3L1-γ is predicted to encode a 252 residues putative protein. We characterized another alternatively spliced isoform, isoform β, which skips exon 5 and encodes a 285 residues putative protein (AY251943, Fig. 3A). A fourth splice variant (NIF3L1-δ; AK023378) with a different 5′-UTR and first ATG codon was also reported (Fig. 3A) (27).

To confirm the interactions between *Wbscr14* and NIF3L1 in mammalian cells, co-immunoprecipitation experiments were carried out in transiently transfected COS-7 (Fig. 3B) and 293T (data not shown) cells with plasmids expressing Myc–EGFP–NIF3L1-α and HA–*Wbscr14*-ζ fusion proteins. Lysates were immunoprecipitated with anti-HA antibodies or anti-*Wbscr14* antisera (7) and probed with anti-GFP specific antibodies. Tagged NIF3L1-α was precipitated exclusively in the presence of HA–*Wbscr14*-ζ, confirming that NIF3L1 and *Wbscr14* interact in mammalian cells (Fig. 3B and C). These results, together with the two-hybrid screen results, indicate that the Wbscr14-interacting domain of NIF3L1 is encoded by the first three exons of the gene.

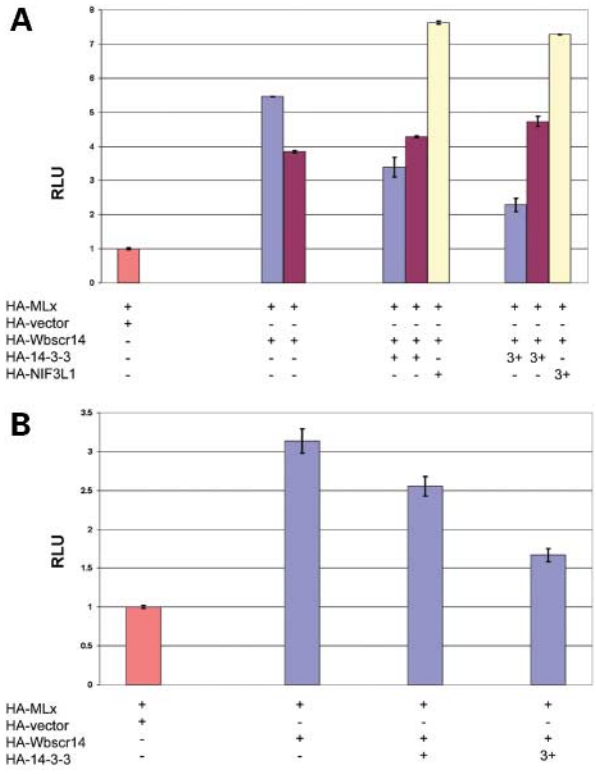

Figure 2. Overexpression of 14-3-3 θ specifically represses transcriptional activity of *Wbscr14*-ζ. (**A**) Relative luciferase units (RLU) of 293T cells transfected with the specified expression plasmids and the pTK81 4 × [E-box]–luciferase reporter. The relative activity of *Wbscr14*-ζ:Mlx (purple) and *Wbscr14*-ζ Δ117–133:Mlx (burgundy) complexes is competed with increasing amounts of 14-3-3 θ, whereas the relative activity of *Wbscr14*-ζ:Mlx upon presence of NIF3L1-α is shown in yellow. For comparison, the corresponding control activity (orange) is indicated. '+' and '3+' signs denote transfections with 400 and 1200 ng of plasmid, respectively. Relative amounts of expressed fusion proteins were assayed by western blotting (data not shown). (**B**) RLU of 293T cells transfected with the specified expression plasmids and the PK(-183)Luc reporter [color code and abbreviations as in (A)].

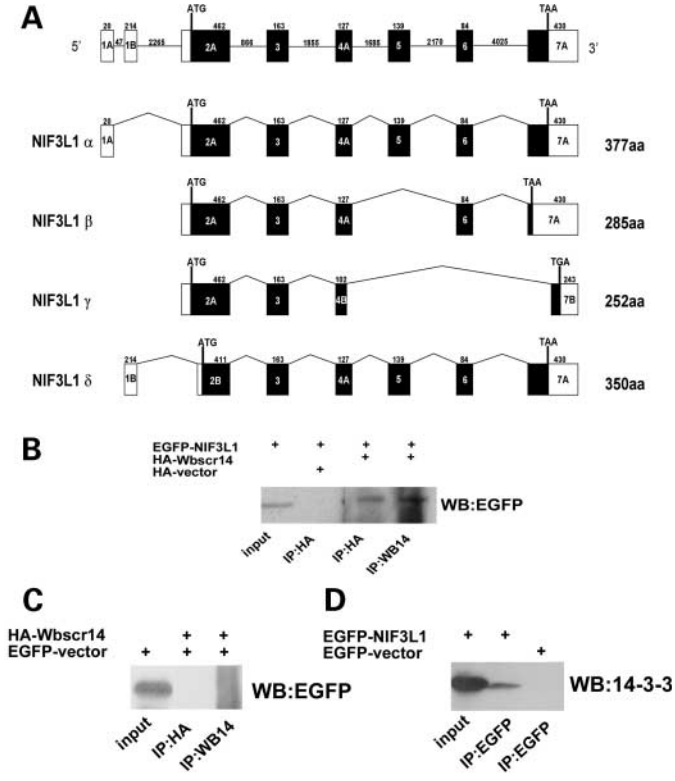

Figure 3. (**A**) Schematic representation of the human *NIF3L1* gene (top) and alternatively spliced transcripts (below). Exons are depicted as filled (coding) and unfilled boxes (5′-and 3′-UTR). The sizes in bp of exons and introns are indicated above, whereas the size in amino acid residues of the putatively encoded proteins are specified on the right. Exons and introns are not to scale. (**B**–**D**) *Wbscr14*, NIF3L1 and 14-3-3 form a complex. COS-7 cells were co-transfected with the specified expression plasmids. Lysates were immunoprecipitated with an anti-HA (IP:HA), an anti-Wbscr14 (IP:WB14) or an anti-GFP antibody (IP:EGFP) and revealed by immunoblotting with an anti-GFP (WB:EGFP) or an anti-14-3-3 antibody (WB:14-3-3).

To determine if *Wbscr14*, 14-3-3 and NIF3L1 are possibly present in a single protein complex, we tried to immunoprecipitate 14-3-3 proteins from Myc–EGFP–NIF3L1-α transfected COS-7 lysates with anti-GFP antibodies. 14-3-3 was immunoprecipitated in the presence of EGFP–NIF3L1, but not in the presence of EGFP alone showing that 14-3-3 interacts with NIF3L1 (Fig. 3C and D). Taken together, these results suggest that WBSCR14:14-3-3:NIF3L1 form a complex in mammalian cells. As expression of 14-3-3 θ leads to the repression of *Wbscr14*-ζ:Mlx-mediated transcription in a dose-dependent manner (see above), we investigated if a similar effect will be obtained upon expression of NIF3L1-α. On the contrary, expression of increasing amounts of NIF3L1 slightly increases the *Wbscr14*-mediated transcriptional activity (Fig. 2A).

Subcellular localization of *Wbscr14*, 14-3-3 and *NIF3L1*

As previously reported, immunofluorescence microscopy shows that *Wbscr14*, 14-3-3 and NIF3L1-α localize in the cytoplasm (5,26,28,29). Similarly, Myc–EGFP–NIF3L1-β and Myc–EGFP–NIF3L1-α–L244X show staining in the cytoplasm of COS-7 cells (Supplementary Material, Fig. S2).

HA–*Wbscr14*-ζ, Myc–EGFP–NIF3L1-α and endogenous 14-3-3 co-localize in the cytoplasm of (co-)transfected 293T, COS-7, HeLa and U2OS cells, providing further evidence that they associate *in vivo* (Supplementary Material, Fig. S3 and data not shown). Mutations of residues S196, S568, S626 and T666 individually or together did not alter the cytoplasmic localization of HA–*Wbscr14*-ζ (Supplementary Material, Fig. S1B and data not shown).

As 14-3-3 proteins promote the cytoplasmic localization of many binding partners by interfering with the function of nuclear localization signals (NLS) or nuclear export sequences (NES) (30), and because high glucose and fatty acids levels were recently shown to regulate the nuclear translocation of the WBSCR14 rat ortholog in primary hepatocytes (6), we investigated if the cytoplasmic localization of *Wbscr14* and NIF3L1 in COS-7 cells was dependent on active nuclear export. Co-transfected COS-7 cells were treated with the CRM1-dependent nuclear export inhibitor Leptomycin B (LMB) (31). The results, as well as examples of subcellular localization, are presented in Figure 4.

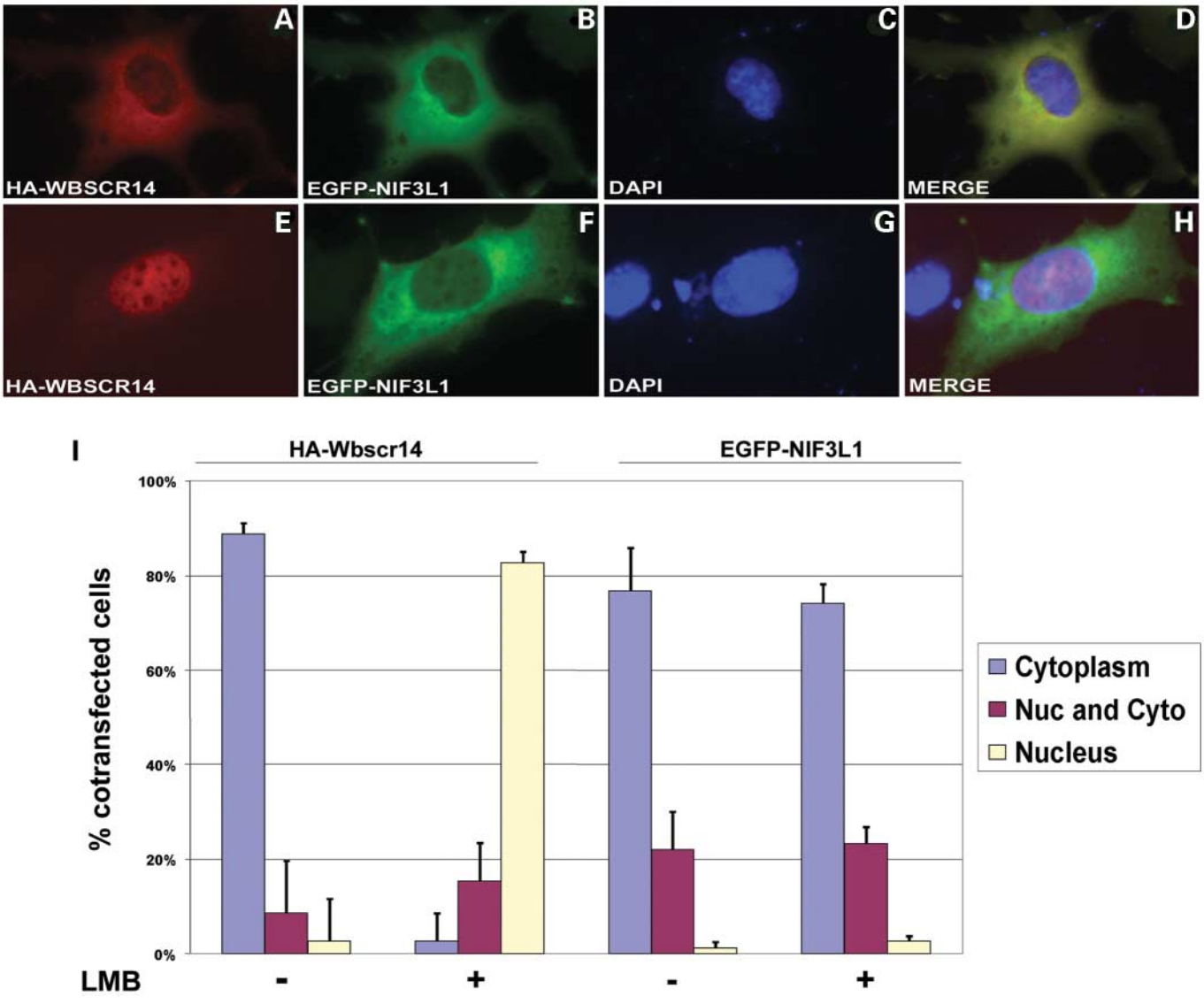

Figure 4. *Wbscr14* is exported actively from the nucleus. (**A**–**H**) Examples of fluorescence microscopy of fixed DAPI-counterstained COS-7 cells transiently co-transfected with HA–*Wbscr14*-ζ and Myc–EGFP–NIF3L1-α mock treated (A–D) or treated with LMB (E–H). EGFP fluorescence: B, D, F and H; staining with anti-HA mAb and AlexaFluor 568-coupled goat anti-mouse antibody: A, D, E and H; DAPI: C, D, G and H. (**I**) Quantification of the subcellular localization of HA–*Wbscr14*-ζ (left) and Myc–EGFP–NIF3L1-α (right) in LMB and mock treated COS-7 cells upon co-transfection of equal amounts of both plasmids. Results are indicated as the percentage of cells expressing fluorescence in the cytoplasm (purple, e.g. A, B and F), the nucleus (pale yellow, e.g. E) and both cellular compartments (burgundy). Please note that upon inhibition of the CRM1 nuclear export pathway *Wbscr14* is retained in the nucleus, whereas NIF3L1 remains cytoplasmic.

A primarily cytoplasmic localization of HA–*Wbscr14*-ζ and Myc–EGFP–NIF3L1-α is shown by 89 ± 6% and 77 ± 4% of COS-7, respectively (Fig. 4A–D and I). Upon treatment with LMB, *Wbscr14* is retained in the nucleus of 83 ± 9% of the analyzed cells. In contrast, the subcellular localization of NIF3L1 remains cytoplasmic (74 ± 9% of cells with a predominantly cytoplasmic signal; Fig. 4E, F, G, H and I). Similar localizations were observed with single transfections (data not shown). These results show that *Wbscr14* shuttles between the cytoplasm and the nucleus, from which it is actively exported, whereas NIF3L1 is uniquely cytoplasmic.

Mapping of the *Wbscr14* NES activity

To map the *Wbscr14* NES activity, we transfected HA-tagged *Wbscr14*-ζ overlapping peptides (Fig. 5A) and analyzed their subcellular distribution in the presence and absence of LMB. The two N-terminal peptides 1–146 and 81–298/PADRE show a cytoplasmic and a nuclear localization in the presence and absence of LMB, respectively, whereas the four other investigated peptides show a predominantly nuclear (272–417; 374–643/MADRE and 584–765/bHLHZip) or predominantly cytoplasmic (737–864/WMC) localization under both conditions (Fig. 5B). These results suggest that either

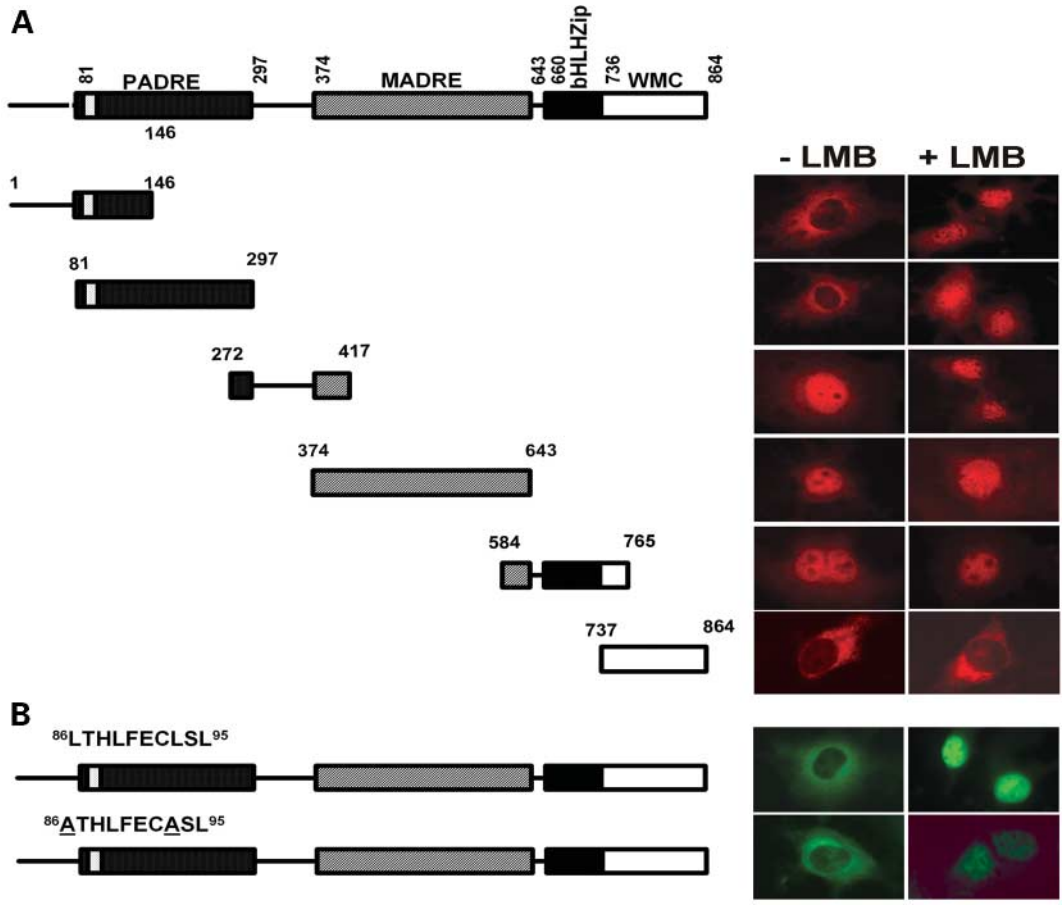

Figure 5. The nuclear export activity of *Wbscr14* maps to the PADRE domain. (**A**) Representative examples of subcellular localization of the HA-tagged *Wbscr14*-ζ peptides schematically depicted on the left in the absence (left column) and presence (right column) of LMB. (**B**) Representative examples of subcellular localization of the Myc–EGFP–*Wbscr14*-ζ, WT and L86A/L93A mutant schematically depicted on the left in the absence (left column) and presence (right column) of LMB.

the *Wbscr14* NES maps between residues 81 and 146 or these residues are forming an interacting-moiety, which allows *Wbscr14* to interact with an NES-containing protein. Furthermore, they indicate that the three peptides 272–417, 374–643/MADRE and 584–765/bHLHZip, either contain an NLS or interact with an NLS-containing protein. Finally, it indicates that the 737–864/WMC peptide holds a section allowing cytoplasmic retention. Consistently, a similar C-terminus portion of MondoA, a WBSCR14 paralog, recently was shown to include a cytoplasmic localization domain (7,23,32). Between residues 81 and 146, the sequence ^{86}LTHLFECLSL^{95} conforms to the NES signature (L-*x*(2,3)-[LIVFM]-*x*(2,3)-L-*x*-[LI]) (33). To confirm that this stretch of residues was participating in the active nuclear export of *Wbscr14*-ζ, we engineered a double mutant by changing two of the characteristic NES signature residues. The Myc–EGFP–*Wbscr14*-ζ, L86A/L93A mutant protein, as its wild-type counterpart, is distributed diffusely in the cytoplasm and nucleus in the absence and presence of LMB, respectively, in the same proportion (Fig. 5B). This indicates that the *Wbscr14* NES-like sequence is not necessary to actively export the protein from the nucleus. This mutant retains its ability to bind 14-3-3 corroborating the previous mapping of the 14-3-3-binding domain of *Wbscr14* to a more distal region of the protein (Fig. 1B and data not shown).

DISCUSSION

The human gene that encodes the WBSCR14 protein maps to 7q11.23, a region commonly deleted in WBS patients. Homozygous deletions of contiguous gene syndrome regions are usually lethal, and in a heterozygote only the dosage-sensitive genes will affect the phenotype. It is thus a challenge to determine which of the WBS hemizygote genes causes the various phenotypes of the syndrome (18,19,34,35). ELN haploinsufficiency has been linked to supravalvular aortic and other stenoses (21,36,37), whereas a mouse model suggests that CYLN2 hemizygosity might contribute to the WBS cognitive profile (38). Furthermore, the study of WBS patients with atypical deletion suggests that *GTF2IRD1*, *GTF2I* and *CYLN2* genes might contribute to the visual spatial processing deficits harbored by WBS patients (39,40). However, the gene(s) responsible for the IGT and

silent diabetes reported in the majority of the WBS patients remains to be determined.

Triglycerides can be synthesized from fatty acids obtained through the diet or produced through *de novo* synthesis from the metabolic intermediate acetyl-CoA. This lipogenesis pathway is regulated by controlling the activity of key enzymes in response to dietary status. This response is thought to be adaptive and occurs in large part through transcriptional regulation of genes encoding lipogenic enzymes (3,41–43). Consistently, in the liver, in response to excess carbohydrate in the diet, the labile WBSCR14, also known as ChREBP binds to the stable Mlx protein to bind E-box elements and activates the transcription of lipogenic genes (5–9,11,14). Inhibition of WBSCR14 activation is therefore expected to attenuate excess fat accumulation resulting from a high-carbohydrate diet. The nuclear translocation of WBSCR14 is controlled by the dephosphorylation of key residues by xylulose 5-phosphate-activated protein phosphatase 2A (5,6,12). To identify proteins, which might participate in the nuclear export/import of WBSCR14, we searched for peptides interacting with the PADRE region, previously shown to repress transcription when fused to a DNA-binding domain (7). In this report, we describe the isolation of five such proteins through two-hybrid selection, four 14-3-3 isotypes and NIF3L1.

The 14-3-3 proteins induce the cytoplasmic translocation and/or retention of its binding partners by masking intrinsic NLSs (e.g. CDC25C) or unmasking intrinsic NESs (e.g. HDAC4 and HDAC5) (44–48). This translocation might be facilitated further through a NES present on the C-termini of 14-3-3 isotypes (49). We showed here that WBSCR14 is exported actively from the nucleus through a CRM1-dependent mechanism in COS-7 cells. This activity was mapped between residues 81 and 146 and is not dependent on the integrity of the WBSCR14 NES-like sequence (residues 86–95). Consistently, the dissection of the function of the different regions of MondoA, a WBSCR14 paralog, using singled-out domains revealed that the region responsible for its cytoplasmic localization resides on its N-terminus (32), a region previously shown to be conserved among WBSCR14, MondoA and their *Caenorhabditis elegans* and *Drosophila melanogaster* orthologs (7). The WBSCR14 export, however, is contingent upon the ability to bind 14-3-3, as expression of increasing amounts of 14-3-3 represses the transcriptional activity of WBSCR14:Mlx complexes in a dose-dependent manner, but not that of heterodimers containing a WBSCR14, which lack the 14-3-3-interaction site (*Wbscr14*-ζ Δ117–133, this work). These results suggest that either WBSCR14 uses the 14-3-3 NES to be exported actively from the nucleus or 14-3-3 creates a link between WBSCR14 and an yet unidentified protein containing an active NES. In many cases, the binding to 14-3-3 and thus the cytoplasmic translocation of the interacting proteins is dependent on their phosphorylation status (50). Consistently, our study shows that the phosphorylation of *Wbscr14*-ζ is important for the 14-3-3-interaction in COS-7 cells. We were unable to identify a specific residue involved in this interaction. Either the engineered alanine mutants at residues 196, 568, 626 and 666 failed to mimic correctly the WBSCR14 dephosphorylated state or the phosphorylation status of an unknown protein is key to bridge 14-3-3 and WBSCR14. Interestingly, the nuclear import/export of WBSCR14 seems to be controlled differently in distinct cells as WBSCR14 alanine mutants translocate to the nucleus in primary rat hepatocytes (6), but fail to do so in COS-7 and 293T cells (Supplementary Material, Fig. S1B).

The shuttling of WBSCR14 between the cytoplasm and the nucleus, as revealed by our LMB assays, is probably under the control of fast export and import processes, to avoid untimed activation of target genes. The 14-3-3 proteins might not only regulate WBSCR14 transcription activity through export control, but also slow down WBSCR14 nuclear entry by masking its NLS or by preventing its dephosphorylation, as shown for the BAD proapoptotic protein (51). However, our observation that the WBSCR14Δ117–133 mutant, which lacks the 14-3-3-interaction moiety, is localized predominantly in the cytoplasm of 293T, COS-7, HeLa and U2OS cells does not support this hypothesis.

In our screen for novel WBSCR14-interactors we also identified NIF3L1. NIF3L1 is the ortholog of the yeast Ngg1-interacting factor 3 (NIF3) (26). The yeast yNIF3p was shown to interact with yNGG1p (52), now designated yADA3p, a subunit of histone acetyltransferase (HAT) complexes (53,54). Reciprocally the human homolog of yADA3p, ADA3, was identified in the PCAF and the hGCN5-containing HAT complexes (55). Moreover, loss of yADA3 or of its partner yADA2 affects transcription of a large number of genes and inhibits the rapid global increase in transcription that occurs in response to glucose, as yeast cells resume rapid growth and accelerate progress through the cell cycle (56). The mouse Nif3l1 protein was shown recently to interact with Trip15/CSN2, a transcriptional corepressor/component of the COP9 signalosome thereby executing a crucial role in retinoic acid-primed neural differentiation of P19 embryonic carcinoma cells (28). Interestingly, the Wbscr14-interacting domain maps to the first 243 residues, whereas the Trip15/CSN2-binding moiety was shown to map to the COOH-terminus (residues 243–376) (this work and 28). These observations suggest that NIF3L1, like its yeast counterpart, functions as a corepressor/coactivator of key transcription regulators complexes. Through immunoprecipitation and subcellular localization, we show that NIF3L1, 14-3-3 and *Wbscr14* are interacting in the cytoplasm of all cell lines tested. Yet in contrast to Wbscr14 and 14-3-3, NIF3L1 does not appear to shuttle between the cytoplasm and the nucleus. Thus, we hypothesized that NIF3L1 might modulate the activity of *Wbscr14*-containing complexes by retaining them in the cytoplasm. Overexpression of NIF3L1 partially increases the *Wbscr14*-mediated transcriptional activity (Fig. 2A). This observation is consistent with the bridge model, where 14-3-3 is necessary to link NIF3L1 and *Wbscr14* and with the ability of NIF3L1 to sequester 14-3-3 in the cytoplasm.

In conclusion, the results presented here indicate that 14-3-3 isotypes (and NIF3L1) regulate the transcriptional activity of *Wbscr14* by modulating its subcellular localization. Hence, 14-3-3 proteins appear to be important regulators of the Mlx-driven transcription factor (this work and 32). The regulation of glucose metabolism by *Wbscr14* supports the hypothesis that the diabetic phenotype observed in WBS patients

could be related to WBSCR14 hemizygosity (5,6,9,14,57). The hemizygosity of this transcription factor could reduce its ability to respond to high-glucose diet through activation of the expression of enzymes involved in *de novo* triglycerides synthesis using glucose precursors. Further experiments will be needed to clarify unambiguously this item.

MATERIALS AND METHODS

Yeast two-hybrid selection

The LexA based yeast two-hybrid selection was performed as described (58). Interaction-mating was used to confirm interaction after isolation of two-hybrid positive clones (25). As judged by western gel analysis of bait fusions with anti-LexA antibody, the engineered *Wbscr14* mutants were expressed to the same level as their wild-type *Wbscr14* counterpart (data not shown).

Genes, mutants and plasmids

Bait plasmids expressing *Wbscr14* peptides fused to the first 202 residues of LexA under the control of the constitutive ADH promoter were created. Wbscr14-ζ cDNA fragments were PCR amplified and cloned directionally in pAR405, a pJG4-5 vector modified to include a new multiple cloning site and no restriction sites after the ADH terminator (58,59). Screening of the human dbEST database with NIF3L1-α allowed to identify ESTs showing skipping of exon 5. The structure of this newly identified isoform, named NIF3L1-β, was confirmed by RT–PCR. Human full-length cDNAs for NIF3L1-α and 14-3-3 θ were RT–PCR amplified from 293T cell RNA. PCR products were cloned into pCDNA3 vectors modified to include either a Myc-tagged EGFP or an HA tag (59). The pCDNA3 HA–*Wbscr14*-ζ and pTK81 4 × [E-box]–luciferase reporter vectors were described previously (7). Deletions to engineer NIF3L1 isoforms from the NIF3L1-α template and missense mutations were generated with the QuickChange site-directed mutagenesis kit (Stratagene) following the manufacturer's protocol. All constructs and mutants were verified by DNA sequencing.

Cell culture and transfection

293T, COS-7, HeLa, U2OS cells (ATCC) were maintained in Dulbecco's modified Eagle's medium (Invitrogen) supplemented with 10% fetal bovine serum (FBS). COS-7, 293T, HeLa and U2OS cells were transfected with Lipofectamine Plus (Invitrogen) or Fugene6 (Roche) according to the manufacturers' instructions.

Immunoprecipitation and western blot

Co-immunoprecipitation experiments were performed as described previously (11,60). Briefly, 48 h post-transfection cells were washed in 1 × phosphate-buffered saline (PBS), and whole-cell lysates were suspended in lysis buffer [1 × PBS, 0.25% NP-40, 1 mM phenylmethylsulfonyl fluoride with Complete Protease Inhibitor Cocktail (Roche)] and incubated on ice for 30 min. Equal amounts of proteins were mixed with the appropriate antibodies and rocked at 4°C overnight. After addition of Protein A–Sepharose or Protein G–Sepharose and incubation for one more hour at 4°C, proteins were immunoprecipitated and washed five times with lysis buffer. Complexes were analyzed by western blotting using anti-GFP polyclonal antibodies (Santa Cruz Biotechnology), anti-HA (12CA5, Roche and BaBCO, Berkeley Antibody Company), or anti-14-3-3 antibodies (H-8 SC-1657, recognizing all 14-3-3 isotypes; C-20 SC-628, C-16 SC-731, T-16 SC-1020, C-16 SC-1019, C-17 SC-732 and C-18 SC-7683 recognizing 14-3-3 isotypes β, γ, ε, ζ, θ and σ, respectively, all from Santa Cruz Biotechnology). Horseradish peroxidase (HRP)-conjugated anti-goat (Santa Cruz Biotechnology), anti-mouse and anti-rabbit antibodies (Amersham-Pharmacia) and the ECL chemiluminescence system (Amersham-Pharmacia) were utilized for detection. For the phosphatase experiment, HA–*Wbscr14* co-immunoprecipitated from transiently transfected COS-7 cells with anti-*Wbscr14* sera and bound to Protein A–Sepharose beads, was washed four times with ice-cold lysis buffer and twice with phosphatase buffer [50 mM Tris–HCl (pH 8.5), 0.1 mM EDTA], resuspended in 50 μl of phosphatase buffer and incubated with or without alkaline phosphatase (20 U/ml; Roche) for 2 h at 37°C. Beads were retrieved by centrifugation and bound proteins eluted by boiling in SDS–PAGE buffer. Separated proteins were transferred to polyvinylidene difluoride (PVDF, Millipore) membranes, soaked in far western solution (1 × PBS, 5% non-fat dry milk, 0.1% Tween) for 1 h at room temperature and incubated overnight at 4°C in far western solution supplemented with 50 μl of rabbit reticulocyte lysate-expressed [^{35}S]Met-labeled 14-3-3 θ produced with the TNT coupled transcription/translation system (Promega). The blot was then washed six times with far western solution without non-fat dry milk, dried and autoradiographed with a Molecular Imager (BioRad).

Subcellular localization

Transfected cells were fixed in 1 × PBS containing 4% formaldehyde for 20 min at room temperature, washed with 1 × PBS, permeabilized with 0.1% Triton X-100 and blocked 1 h with PBS/1% bovine serum albumin (BSA). The anti-HA antibody and the secondary anti-mouse AlexaFluor 568 (Molecular Probes) were used at 1:1000 and 1:500 dilutions, respectively. Cells were incubated for 1 h with the primary antibody at room temperature. After extensive washing with PBS, cells were incubated for 1 h at room temperature with secondary antibody. Nuclei were stained with DAPI (1 μg/ml). To quantify subcellular localization, independent transfections were carried out at least three times, and not less than 100 cells were counted for each transfection. In co-transfections, only cells expressing both proteins were scored. For shuttling experiments, cells were treated with 10 ng/ml LMB for 12 h (61).

Transcription assays

An amount of 2.0×10^5 293T cells were co-transfected with 400 ng of pCDNA3 HA–*Wbscr14*-ζ wild-type or mutant,

400 ng of pCDNA3 HA–Mlx, 950 ng of pTK81 4 × [E-box]–luciferase reporter (7) or PK(-183)Luc (62) and 400 or 1200 ng of pCDNA3 HA–14-3-3 θ. Fifty nanograms of pRL-SV40 (Promega) and Salmon sperm were added to measure transfection efficiency and to balance the quantity of final DNA, respectively. After 36 h post-transfection, cells were harvested and luciferase activity was measured by dual luciferase reporter assay system following the manufacturer protocol (Promega). The results are expressed as the relative luciferase activity of the appropriate control. The experiments were carried out three times in triplicate.

SUPPLEMENTARY MATERIAL

Supplementary Material is available at HMG Online.

ACKNOWLEDGEMENTS

We thank S. Deutsch for helpful suggestions and critical reading of the manuscript and C. Rossier and C. Ucla for assistance. We are grateful to M. Yoshida for Leptomycin B and to R. Brent, J. Gyuris, D. Krainc and H. Towle for plasmids and/or libraries. This work was supported by grants from the Telethon Action Suisse Foundation, the Jérôme Lejeune Foundation, the Swiss Cancer League and the Swiss National Science Foundation to A.R., and by a FIRC (Fondazione Italiana per la Ricerca sul Cancro) fellowship to G.M.

REFERENCES

1. Goodridge, A.G. (1987) Dietary regulation of gene expression: enzymes involved in carbohydrate and lipid metabolism. *Annu. Rev. Nutr.*, **7**, 157–185.
2. Granner, D. and Pilkis, S. (1990) The genes of hepatic glucose metabolism. *J. Biol. Chem.*, **265**, 10173–10176.
3. Towle, H.C., Kaytor, E.N. and Shih, H.M. (1997) Regulation of the expression of lipogenic enzyme genes by carbohydrate. *Annu. Rev. Nutr.*, **17**, 405–433.
4. Wain, H.M., Bruford, E.A., Lovering, R.C., Lush, M.J., Wright, M.W. and Povey, S. (2002) Guidelines for human gene nomenclature. *Genomics*, **79**, 464–470.
5. Kawaguchi, T., Takenoshita, M., Kabashima, T. and Uyeda, K. (2001) Glucose and cAMP regulate the L-type pyruvate kinase gene by phosphorylation/dephosphorylation of the carbohydrate response element binding protein. *Proc. Natl Acad. Sci. USA*, **98**, 13710–13715.
6. Uyeda, K., Yamashita, H. and Kawaguchi, T. (2002) Carbohydrate responsive element-binding protein (ChREBP): a key regulator of glucose metabolism and fat storage. *Biochem. Pharmacol.*, **63**, 2075–2080.
7. Cairo, S., Merla, G., Urbinati, F., Ballabio, A. and Reymond, A. (2001) *WBSCR14*, a gene mapping to the Williams–Beuren syndrome deleted region, is a new member of the Mlx transcription factor network. *Hum. Mol. Genet.*, **10**, 617–627.
8. de Luis, O., Valero, M.C. and Jurado, L.A. (2000) WBSCR14, a putative transcription factor gene deleted in Williams–Beuren syndrome: complete characterisation of the human gene and the mouse ortholog. *Eur. J. Hum. Genet.*, **8**, 215–222.
9. Yamashita, H., Takenoshita, M., Sakurai, M., Bruick, R.K., Henzel, W.J., Shillinglaw, W., Arnot, D. and Uyeda, K. (2001) A glucose-responsive transcription factor that regulates carbohydrate metabolism in the liver. *Proc. Natl Acad. Sci. USA*, **98**, 9116–9121.
10. Zhou, Z.Q. and Hurlin, P.J. (2001) The interplay between Mad and Myc in proliferation and differentiation. *Trends Cell Biol.*, **11**, S10–S14.
11. Meroni, G., Cairo, S., Merla, G., Messali, S., Brent, R., Ballabio, A. and Reymond, A. (2000) Mlx, a new Max-like bHLHZip family member: the center stage of a novel transcription factors regulatory pathway? *Oncogene*, **19**, 3266–3277.
12. Kabashima, T., Kawaguchi, T., Wadzinski, B.E. and Uyeda, K. (2003) Xylulose 5-phosphate mediates glucose-induced lipogenesis by xylulose 5-phosphate-activated protein phosphatase in rat liver. *Proc. Natl Acad. Sci. USA*, **8**, 5107–5112.
13. Stoeckman, A.K. and Towle, H.C. (2002) The role of SREBP-1c in nutritional regulation of lipogenic enzyme gene expression. *J. Biol. Chem.*, **277**, 27029–27035.
14. Stoeckman, A.K., Ma, L. and Towle, H.C. (2004) Mlx is the functional heteromeric partner of ChREBP in glucose regulation of lipogenic enzyme genes. *J. Biol. Chem.*, **207**, 15662–15669.
15. Meng, X., Lu, X., Li, Z., Green, E.D., Massa, H., Trask, B.J., Morris, C.A. and Keating, M.T. (1998) Complete physical map of the common deletion region in Williams syndrome and identification and characterization of three novel genes. *Hum. Genet.*, **103**, 590–599.
16. Morris, C.A., Demsey, S.A., Leonard, C.O., Dilts, C. and Blackburn, B.L. (1988) Natural history of Williams syndrome: physical characteristics. *J. Pediatr.*, **113**, 318–326.
17. Pober, B.R., Wang, E., Petersen, K., Osborne, L. and Caprio, S. (2001) Impaired glucose tolerance in Williams syndrome. *Am. J. Hum. Genet.*, **69**, S302.
18. Francke, U. (1999) Williams–Beuren syndrome: genes and mechanisms. *Hum. Mol. Genet.*, **8**, 1947–1954.
19. Osborne, L.R. (1999) Williams–Beuren syndrome: unraveling the mysteries of a microdeletion disorder. *Mol. Genet. Metab.*, **67**, 1–10.
20. Osborne, L.R., Li, M., Pober, B., Chitayat, D., Bodurtha, J., Mandel, A., Costa, T., Grebe, T., Cox, S., Tsui, L.C. *et al.* (2001) A 1.5 million-base pair inversion polymorphism in families with Williams–Beuren syndrome. *Nat. Genet.*, **29**, 321–325.
21. Ewart, A.K., Morris, C.A., Atkinson, D., Jin, W., Sternes, K., Spallone, P., Stock, A.D., Leppert, M. and Keating, M.T. (1993) Hemizygosity at the elastin locus in a developmental disorder, Williams syndrome. *Nat. Genet.*, **5**, 11–16.
22. Perez Jurado, L.A. (2003) Williams–Beuren syndrome: a model of recurrent genomic mutation. *Horm. Res.*, **59**, S106–S113.
23. Billin, A.N., Eilers, A.L., Coulter, K.L., Logan, J.S. and Ayer, D.E. (2000) MondoA, a novel basic helix-loop-helix-leucine zipper transcriptional activator that constitutes a positive branch of a max-like network. *Mol. Cell. Biol.*, **20**, 8845–8854.
24. Yaffe, M.B. (2002) How do 14-3-3 proteins work? Gatekeeper phosphorylation and the molecular anvil hypothesis. *FEBS Lett.*, **513**, 53–57.
25. Reymond, A. and Brent, R. (1995) p16 proteins from melanoma-prone families are deficient in binding to Cdk4. *Oncogene*, **11**, 1173–1178.
26. Tascou, S., Uedelhoven, J., Dixkens, C., Nayernia, K., Engel, W. and Burfeind, P. (2000) Isolation and characterization of a novel human gene, *NIF3L1*, and its mouse ortholog, *Nif3l1*, highly conserved from bacteria to mammals. *Cytogenet. Cell Genet.*, **90**, 330–336.
27. Tascou, S., Kang, T.W., Trappe, R., Engel, W. and Burfeind, P. (2003) Identification and characterization of NIF3L1 BP1, a novel cytoplasmic interaction partner of the NIF3L1 protein. *Biochem. Biophys. Res. Commun.*, **309**, 440–448.
28. Akiyama, H., Fujisawa, N., Tashiro, Y., Takanabe, N., Sugiyama, A. and Tashiro, F. (2003) The role of transcriptional corepressor Nif3l1 in early stage of neural differentiation via cooperation with Trip15/CSN2. *J. Biol. Chem.*, **278**, 10752–10762.
29. Fu, H., Subramanian, R.R. and Masters, S.C. (2000) 14-3-3 proteins: structure, function, and regulation. *Annu. Rev. Pharmacol. Toxicol.*, **40**, 617–647.
30. Muslin, A.J. and Xing, H. (2000) 14-3-3 proteins: regulation of subcellular localization by molecular interference. *Cell Signal.*, **12**, 703–709.
31. Kudo, N., Matsumori, N., Taoka, H., Fujiwara, D., Schreiner, E.P., Wolff, B., Yoshida, M. and Horinouchi, S. (1999) Leptomycin B inactivates CRM1/exportin 1 by covalent modification at a cysteine residue in the central conserved region. *Proc. Natl Acad. Sci. USA*, **96**, 9112–9117.
32. Eilers, A.L., Sundwall, E., Lin, M., Sullivan, A.A. and Ayer, D.E. (2002) A novel heterodimerization domain, CRM1, and 14-3-3 control subcellular localization of the MondoA-Mlx heterocomplex. *Mol. Cell. Biol.*, **22**, 8514–8526.

33. la Cour, T., Gupta, R., Rapacki, K., Skriver, K., Poulsen, F.M. and Brunak, S. (2003) NESbase version 1.0: a database of nuclear export signals. *Nucl. Acids Res.*, **31**, 393–396.
34. Merla, G., Ucla, C., Guipponi, M. and Reymond, A. (2002) Identification of additional transcripts in the Williams–Beuren syndrome critical region. *Hum. Genet.*, **110**, 429–438.
35. Doll, A. and Grzeschik, K.H. (2001) Characterization of two novel genes, *WBSCR20* and *WBSCR22*, deleted in Williams–Beuren syndrome. *Cytogenet. Cell Genet.*, **95**, 20–27.
36. Tassabehji, M., Metcalfe, K., Donnai, D., Hurst, J., Reardon, W., Burch, M. and Read, A.P. (1997) Elastin: genomic structure and point mutations in patients with supravalvular aortic stenosis. *Hum. Mol. Genet.*, **6**, 1029–1036.
37. Li, T., Narhi, L.O., Wen, J., Philo, J.S., Sitney, K., Inoue, J., Yamamoto, T. and Arakawa, T. (1998) Interactions between NFkappaB and its inhibitor ikappaB: biophysical characterization of a NFkappaB/ikappaB-alpha complex. *J. Protein Chem.*, **17**, 757–763.
38. Hoogenraad, C.C., Koekkoek, B., Akhmanova, A., Krugers, H., Dortland, B., Miedema, M., van Alphen, A., Kistler, W.M., Jaegle, M., Koutsourakis, M. *et al.* (2002) Targeted mutation of Cyln2 in the Williams syndrome critical region links CLIP-115 haploinsufficiency to neurodevelopmental abnormalities in mice. *Nat. Genet.*, **32**, 116–127.
39. Hirota, H., Matsuoka, R., Chen, X.N., Salandanan, L.S., Lincoln, A., Rose, F.E., Sunahara, M., Osawa, M., Bellugi, U. and Korenberg, J.R. (2003) Williams syndrome deficits in visual spatial processing linked to GTF2IRD1 and GTF2I on chromosome 7q11.23. *Genet. Med.*, **5**, 311–321.
40. Gagliardi, C., Bonaglia, M.C., Selicorni, A., Borgatti, R. and Giorda, R. (2003) Unusual cognitive and behavioural profile in a Williams syndrome patient with atypical 7q11.23 deletion. *J. Med. Genet.*, **40**, 526–530.
41. Girard, J., Ferre, P. and Foufelle, F. (1997) Mechanisms by which carbohydrates regulate expression of genes for glycolytic and lipogenic enzymes. *Annu. Rev. Nutr.*, **17**, 325–352.
42. Hillgartner, F.B., Salati, L.M. and Goodridge, A.G. (1995) Physiological and molecular mechanisms involved in nutritional regulation of fatty acid synthesis. *Physiol. Rev.*, **75**, 47–76.
43. Vaulont, S., Vasseur-Cognet, M. and Kahn, A. (2000) Glucose regulation of gene transcription. *J. Biol. Chem.*, **275**, 31555–31558.
44. Dalal, S.N., Schweitzer, C.M., Gan, J. and DeCaprio, J.A. (1999) Cytoplasmic localization of human cdc25C during interphase requires an intact 14-3-3 binding site. *Mol. Cell. Biol.*, **19**, 4465–4479.
45. Wang, A.H., Kruhlak, M.J., Wu, J., Bertos, N.R., Vezmar, M., Posner, B.I., Bazett-Jones, D.P. and Yang, X.J. (2000) Regulation of histone deacetylase 4 by binding of 14-3-3 proteins. *Mol. Cell. Biol.*, **20**, 6904–6912.
46. Yang, J., Winkler, K., Yoshida, M. and Kornbluth, S. (1999) Maintenance of G2 arrest in the Xenopus oocyte: a role for 14-3-3-mediated inhibition of Cdc25 nuclear import. *EMBO J.*, **18**, 2174–2183.
47. McKinsey, T.A., Zhang, C.L. and Olson, E.N. (2001) Identification of a signal-responsive nuclear export sequence in class II histone deacetylases. *Mol. Cell. Biol.*, **21**, 6312–6321.
48. Grozinger, C.M. and Schreiber, S.L. (2000) Regulation of histone deacetylase 4 and 5 and transcriptional activity by 14-3-3-dependent cellular localization. *Proc. Natl Acad. Sci. USA*, **97**, 7835–7840.
49. Lopez-Girona, A., Furnari, B., Mondesert, O. and Russell, P. (1999) Nuclear localization of Cdc25 is regulated by DNA damage and a 14-3-3 protein. *Nature*, **397**, 172–175.
50. Mils, V., Baldin, V., Goubin, F., Pinta, I., Papin, C., Waye, M., Eychene, A. and Ducommun, B. (2000) Specific interaction between 14–3-3 isoforms and the human CDC25B phosphatase. *Oncogene*, **19**, 1257–1265.
51. Chiang, C.W., Harris, G., Ellig, C., Masters, S.C., Subramanian, R., Shenolikar, S., Wadzinski, B.E. and Yang, E. (2001) Protein phosphatase 2A activates the proapoptotic function of BAD in interleukin-3-dependent lymphoid cells by a mechanism requiring 14–3-3 dissociation. *Blood*, **97**, 1289–1297.
52. Martens, J.A., Genereaux, J., Saleh, A. and Brandl, C.J. (1996) Transcriptional activation by yeast PDR1p is inhibited by its association with NGG1p/ADA3p. *J. Biol. Chem.*, **271**, 15884–15890.
53. Sterner, D.E., Grant, P.A., Roberts, S.M., Duggan, L.J., Belotserkovskaya, R., Pacella, L.A., Winston, F., Workman, J.L. and Berger, S.L. (1999) Functional organization of the yeast SAGA complex: distinct components involved in structural integrity, nucleosome acetylation, and TATA- binding protein interaction. *Mol. Cell. Biol.*, **19**, 86–98.
54. Grant, P.A., Sterner, D.E., Duggan, L.J., Workman, J.L. and Berger, S.L. (1998) The SAGA unfolds: convergence of transcription regulators in chromatin- modifying complexes. *Trends Cell Biol.*, **8**, 193–197.
55. Ogryzko, V.V., Kotani, T., Zhang, X., Schiltz, R.L., Howard, T., Yang, X.J., Howard, B.H., Qin, J. and Nakatani, Y. (1998) Histone-like TAFs within the PCAF histone acetylase complex. *Cell*, **94**, 35–44.
56. Wu, M., Newcomb, L. and Heideman, W. (1999) Regulation of gene expression by glucose in *Saccharomyces cerevisiae*: a role for ADA2 and ADA3/NGG1. *J. Bacteriol.*, **181**, 4755–4760.
57. Kawaguchi, T., Osatomi, K., Yamashita, H., Kabashima, T. and Uyeda, K. (2002) Mechanism for fatty acid 'sparing' effect on glucose-induced transcription: regulation of carbohydrate-responsive element-binding protein by AMP-activated protein kinase. *J. Biol. Chem.*, **277**, 3829–3835.
58. Gyuris, J., Golemis, E., Chertkov, H. and Brent, R. (1993) Cdi1, a human G1 and S phase protein phosphatase that associates with Cdk2. *Cell*, **75**, 791–803.
59. Reymond, A., Meroni, G., Fantozzi, A., Merla, G., Cairo, S., Luzi, L., Riganelli, D., Zanaria, E., Messali, S., Cainarca, S. *et al.* (2001) The tripartite motif family identifies cell compartments. *EMBO J.*, **20**, 2140–2151.
60. Reymond, A., Volorio, S., Merla, G., Al-Maghtheh, M., Zuffardi, O., Bulfone, A., Ballabio, A. and Zollo, M. (1999) Evidence for interaction between human PRUNE and nm23-H1 NDPKinase. *Oncogene*, **18**, 7244–7252.
61. Akakura, S., Yoshida, M., Yoneda, Y. and Horinouchi, S. (2001) A role for Hsc70 in regulating nucleocytoplasmic transport of a temperature-sensitive p53 (p53Val-135). *J. Biol. Chem.*, **276**, 14649–14657.
62. Kaytor, E.N., Shih, H. and Towle, H.C. (1997) Carbohydrate regulation of hepatic gene expression. Evidence against a role for the upstream stimulatory factor. *J. Biol. Chem.*, **272**, 7525–7531.